Giant magnetocaloric effect for (Mn, Fe, V)2(P, Si) alloys with low hysteresis

Lai, Jiawei; Huang, Bowei; You, Xinmin; Maschek, Michael; Zhou, Guofu; van Dijk, Niels; Brück, Ekkes

DOI
10.1016/j.jsamd.2023.100660

Publication date
2024

Published in
Journal of Science: Advanced Materials and Devices

Citation (APA)
Lai, J., Huang, B., You, X., Maschek, M., Zhou, G., van Dijk, N., & Brück, E. (2024). Giant magnetocaloric effect for (Mn, Fe, V)2(P, Si) alloys with low hysteresis. *Journal of Science: Advanced Materials and Devices*, *9*(1), Article 100660. https://doi.org/10.1016/j.jsamd.2023.100660

Journal of Science: Advanced Materials and Devices 9 (2024) 100660

Contents lists available at ScienceDirect

Journal of Science: Advanced Materials and Devices

journal homepage: www.elsevier.com/locate/jsamd

Giant magnetocaloric effect for (Mn, Fe, V)2(P, Si) alloys with low hysteresis

Jiawei Lai [a,b,*], Bowei Huang [b], Xinmin You [b], Michael Maschek [b], Guofu Zhou [a], Niels van Dijk [b], Ekkes Brück [b]

[a] Guangdong Provincial Key Laboratory of Optical Information Materials and Technology, Institute of Electronic Paper Displays, South China Academy of Advanced Optoelectronics, South China Normal University, Guangzhou, 510006, PR China

[b] Fundamental Aspects of Materials and Energy, Department of Radiation Science and Technology, TU Delft, Mekelweg 15, 2629JB Delft, the Netherlands

ARTICLE INFO

Keywords:
$(Mn,Fe)_2(P,Si)$ alloy
Magnetocaloric effect
Hysteresis
Crystal structure evolution
Isothermal entropy change
Adiabatic temperature change

ABSTRACT

The Fe_2P type Mn–Fe–P–Si alloys exhibit a giant magneto-elastic first-order transition, but the large hysteresis limits their performance. Crystal structure evolution and magnetocaloric performance were investigated by varying the Mn and Fe contents at a constant V substitution of 0.02 in Fe_2P-type $(Mn_{1.17-x}Fe_{0.73-y}V_{0.02})$ $(P_{0.5}Si_{0.5})$ (where $x + y = 0.02$). The V substitution of Fe content shows a larger reduction of hysteresis compared with the same substitution amount of Mn content. During magnetoelastic phase transition, V-substitution reduces the volume change and the volumetric stresses, providing a superior mechanical stability. Compound with the V substitution of Fe ($y = 0.02$) shows the best magnetocaloric effect with a low thermal hysteresis of 0.6 K. Our developed $Mn_{1.17-x}Fe_{0.73-y}V_{0.02}P_{0.5}Si_{0.5}$ alloys are excellent materials for room-temperature magnetic heat-pumping applications by using a permanent magnet.

1. Introduction

The need to realise a worldwide reduction in carbon emissions provides the motivation to develop environmentally friendly cooling technologies. In comparison to the vapour gas-compression refrigeration, magnetic heat-pumping near room-temperature is regarded to be an alternative technology due to its high energy efficiency and environmentally friendly solid-state cooling materials. The magnetic heat pump technology utilizes the magnetic field induced temperature change, which is based on the magnetocaloric effect (MCE). In order to achieve a giant MCE, a few promising material families with a first-order magnetic transition (FOMT) have been developed, such as $Gd_5Ge_2Si_2$ [1], $LaFe_{13-x}Si_x$ [2],2 [3], MnFe(P,As/Si) [4,5], Mn-Co-Ge [6] and Heusler [7] compounds. The Mn–Fe–P–Si alloys are regarded as one of the materials families that have the potential to be industrialized due to their abundant starting materials, tunable Curie temperature (T_C) and outstanding MCE [8].

The large hysteresis in the strong FOMT Mn–Fe–P–Si alloys restricts the efficiency in the application of these materials [9,10]. A well-known strategy is to tune the phase transition to the border of the FOMT to the second-order magnetic transition (SOMT). Different methods have been attempted to tune the FOMT to a SOMT by changing the stoichiometry [11], varying the annealing temperature [12,13], chemical substitution with elements such as Ni, Co, Cu [14,15], or introducing interstitial atoms like B, C, N [16–18]. However, these approaches generally weaken the FOMT and reduce the magnetic entropy change (ΔS_M) of the FOMT.

Since permanent magnets are widely used as applied magnetic field sources in the devices [19,20], generating a limited field from 0.8 to 1.93 T, it is of particular interest to systematically investigate the field induced MEC within this field range. One of the solutions is to increase the value of dT_C/dB to obtain a larger ΔS_M under the same strength of the magnetic field. The shift of the transition temperature in magnetic fields dTc/dB, which is positive for a conventional first-order transition, can be regarded as the driving force of the magnetocaloric effect in such a material. Improving the dTc/dB suggests that the phase transition is induced in a lower magnetic field. From the Clausius-Clapeyron relation [21], dT_C/dB can be enlarged when the total entropy change (ΔS) is

Peer review under responsibility of Vietnam National University, Hanoi.

* Corresponding author. Guangdong Provincial Key Laboratory of Optical Information Materials and Technology, Institute of Electronic Paper Displays, South China Academy of Advanced Optoelectronics, South China Normal University, Guangzhou, 510006, PR China.

E-mail address: jiawei.lai@m.scnu.edu.cn (J. Lai).

https://doi.org/10.1016/j.jsamd.2023.100660

Received 16 August 2023; Received in revised form 22 November 2023; Accepted 1 December 2023

Available online 6 December 2023

Table 1
List of T_C, ΔT_{hys}, the latent heat L and entropy change ΔS_L, $|\Delta S_M|$ and ΔT_{ad} under a magnetic field change of 1 T for $Mn_{1.17-x}Fe_{0.73-y}V_{0.02}P_{0.5}Si_{0.5}$ alloys.

Sample Number	*Sample* Compositions	T_C (K)	ΔT_{hys} (K)	L (kJ/kg)	$\|\Delta S_M\|$ (J/(kg·K))	ΔT_{ad} (K)	ΔS_L (J/K)
M0F0	*x=0.00, y=0.00*	311.2	1.5	9.3	8.7	2.4	29.9
M0F2	*x=0.00, y=0.02*	290.1	0.6	6.3	9.2	3.0	21.8
M1F1	*x=0.01, y=0.01*	293.3	1.0	7.3	8.9	2.4	24.9
M2F0	*x=0.02, y=0.00*	293.1	1.2	7.1	8.5	2.8	24.3
Ref. [8]	Mn–Fe–P–Si–B	281.2	2.0	3.8	9.8	2.5	13.5

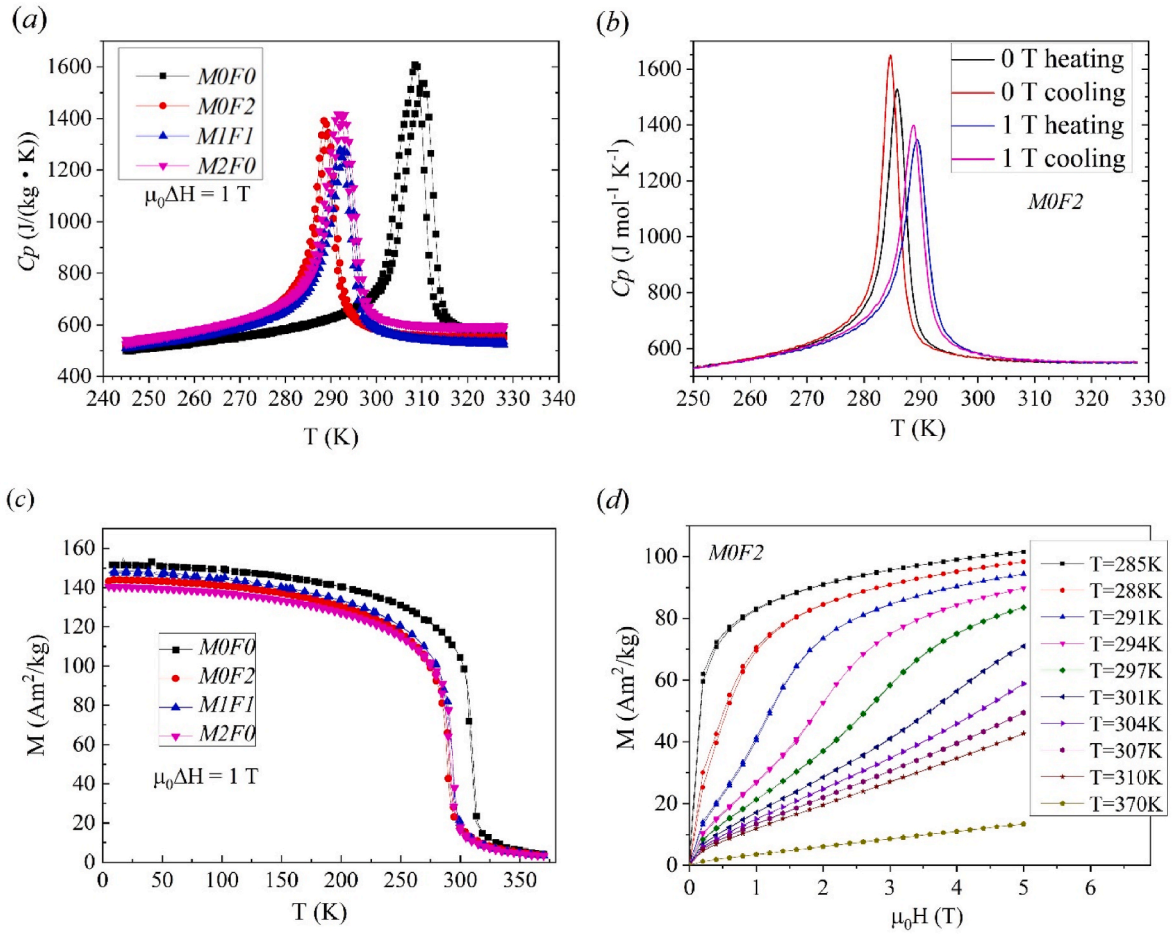

Fig. 1. (*a*) Heat capacity under a magnetic field of 1 T for all samples and (*b*) Heat capacity under a magnetic field of 0 and 1 T for *M0F2*; (*c*) Magnetization as a function of temperature under a magnetic field of 1 T for all samples; (*d*) Magnetization as a function of temperature for *M0F2*.

reduced and ΔM is conserved. Interstitial boron has been reported to have a significant effect on increasing dT_C/dB, which increases from 2.1 to 4.5 K/T when adding boron [22]. However, the non-metallic elements like B may reduce the thermal conductivity of the Mn–Fe–P–Si alloys. Therefore, a metallic element is preferred. In previous experiments, V substitution for Mn or Fe demonstrated that it was feasible to decrease the hysteresis and have a better MCE under a low applied magnetic field (<1.2T). And the optimal amount of substitution is determined to be 0.02 [13,23]. However, a comprehensive investigation of the phase evolution during phase transition, the ΔS_M, and adiabatic temperature change (ΔT_{ad}) is not revealed yet. Typically, stoichiometry of Fe_2P-type alloys needs to be optimize depending on the raw powders used in the powder metallurgy process. Based on our previous experiments, we determined a stoichiometric of 1.92 instead of an algebraic integer value of 2.0, i.e. $(Mn, Fe)_{1.92}(P, Si)$ to suppress the impurity. In this work, we vary the Mn and Fe contents at a fixed V substitution in the novel Fe_2P-type $(Mn_{1.17-x}Fe_{0.73-y}V_{0.02})(P_{0.5}Si_{0.5})$ (where $x + y = 0.02$) alloys, and systematically investigated the phase evolution and magnetocaloric performance (ΔS_M and ΔT_{ad}) during FOMT.

2. Experimental

Polycrystalline $(Mn_{1.17-x}Fe_{0.73-y}V_{0.02})(P_{0.5}Si_{0.5})$ alloys ($x + y = 0.02$) were prepared by a powder metallurgy method. The starting materials in the form of Mn (99.7 %), Fe (99.7 %), red P (99 %), Si (99.7 %) and V (99.5 %) powders were mechanically ball milled for 10 h with a constant rotation speed of 380 rpm in Ar, then pressed into small pellets, and finally sealed in quartz ampoules under 200 mbar of Ar. These pellets were annealed at 1373 K for 20 h to homogenize the compound and finally quenched in water. The sample ($x = 0.00$, $y = 0.00$) is coded as *M0F0*. Other samples like ($x = 0.00$, $y = 0.02$), ($x = 0.01$, $y = 0.01$), ($x = 0.02$, $y = 0.00$) are coded as *M0F2*, *M1F1* and *M2F0*, as listed in Table 1. Tablets of the $Mn_{1.17-x}Fe_{0.73-y}V_{0.02}P_{0.5}Si_{0.5}$ alloys are prepared as describe previously [16]. These tablets were annealed at 1373 K for 25 h

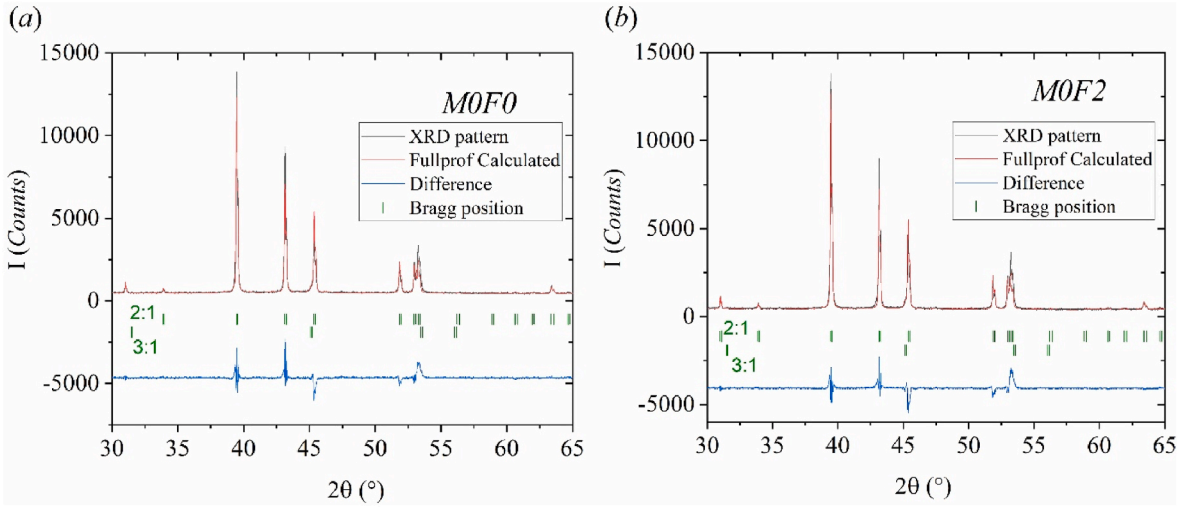

Fig. 2. Rietveld refinement for XRD patterns of *M0F0* and *M0F2* measured at 373 K.

and quenched in water.

X-ray diffraction (XRD) patterns were measured on a PANalytical X-pert Pro diffractometer with Cu-Kα radiation (1.54056 Å). The temperature dependence and magnetic field dependence of the magnetization were measured with a commercial superconducting quantum interference device (SQUID) magnetometer (Quantum Design MPMS 5XL). The adiabatic temperature change (ΔTad) was measured in a Peltier cell based differential scanning calorimeter (DSC) using a Halbach cylinder providing a magnetic field of up to 1.5 T. Direct ΔTad vales were measured from home-build device, where the materials are reciprocating moving in a permanent magnetic array of 1.1 T. The measured samples are grinded to powder particles with a size <150 μm. Samples are measured in a device with an applied magnetic field varying between 0 and 1.1 T. As reference sample, Gd spheres in the size range of 400–800 μm are also measured at the same time.

3. Results and discussion

Fig. 1(*a*) shows the differential scanning calorimeter (DSC) results measured by a TA-Q2000 instrument at a rate of 3 K/min. The latent heat (L) values, which are integration of DSC heating curves under zero field with a linear background subtraction, are 9.3, 6.3, 7.3, 7.1 kJ/kg for *M0F0*, *M0F2*, *M1F1* and *M2F0,* respectively. From the above, value of L is reduced by the V substitution. The values of ΔS_L are calculated by $\Delta S_L = L/T_c$ is 29.9, 21.8, 24.9 and 24.3 J/K for *M0F0*, *M0F2*, *M1F1* and *M2F0,* respectively. The value of L can be regarded as a sign of the strength of the FOMT. Thus, the strength of FOMT can be maximally reduced by 32 % with a V substitution of 0.02 in *M0F2*. The trend of ΔS_L is consistent with the data under a larger field of 1.5 T, indicating 1.5 T is sufficient to fully induce the FOMT. The V substitution of 0.02 decreases the ΔS_L only slightly, and thereby retains the giant MCE. Fig. 1(*b*) illustrates the DSC patterns for the *M0F2* alloy for magnetic fields of 0 and 1 T during heating and cooling. The value of $dTc/d\mathrm{B}$ is 4.1 K/T, which is comparable to the Mn–Fe–P–Si–B alloys [22]. Thus, the $Mn_{1.17-x}Fe_{0.73-y}V_{0.02}P_{0.5}Si_{0.5}$ alloys are expected to have a superior low field MCE. The hysteresis can be determined from the C_p peak during heating and cooling and amounts to 1.2 and 0.6 K in magnetic fields of 0 and 1 T, respectively. A low hysteresis of 0.6 K provides a high cooling cycle efficiency, as suggested by Brown et al. [9] Hysteresis is reduced when applied a magnetic field since the external field source provide an additional energy to cross the energy barrier of FOMT. Consequently, thermal hysteresis is 1.2 K at zero magnetic field, but it reduces to 0.6 K under a magnetic field of 1 T.

The magnetization as a function of temperature for the $Mn_{1.17-x}Fe_{0.73-y}V_{0.02}P_{0.5}Si_{0.5}$ alloys in a magnetic field of 1 T is shown in Fig. 1 (*c*). The magnetization values are 151.7, 147.5, 144.0, 140.4 Am^2/kg and the values of T_C are 311.2, 290.1, 293.3 and 293.1 K for sample *M0F0*, *M0F2*, *M1F1* and *M2F0*, respectively. The magnetization is reduced linearly with the reduction in Mn, which can be related to the high magnetic moment of Mn(*3g*) [24]. The different replacements of 0.02 of Fe and Mn result in a variation in T_C of 3.2 K. However, the -*dM/dT* values are 9.7, 10.8, 8.8, 9.2 Am^2/kgK for the *M0F0*, *M0F2*, *M1F1* and *M2F0*, respectively. -*dM/dT* for the *M0F2* alloy is larger than the one without V. This increase is astonishing since thermal hysteresis (ΔT_{hys}) decreases from 1.5 to 0.6 K from *M0F0* to *M0F2*. The unusual -*dM/dT* increase is attributing to a steeper field dependence at 1 T, which indicates a stronger first order magnetoelastic coupling. *M0F2* is therefore concluded to be the optimal V substitution in this work. Its structure and properties will be investigated in the next section.

The ΔT_{hys} is calculated from the temperature difference in the maximum of -*dM/dT* between heating and cooling in the *M-T* curves in a magnetic field of 1 T, as shown in Table 1. Interestingly, thermal hysteresis can be manipulated by tuning V substitution with Fe or Mn. For instance, compared to zero V content, ΔT_{hys} for M0F2 shows a reduction of 0.9 K and ΔT_{hys} for M2F0 shows a reduction of 0.3 K. In other words, 0.02 substitution of Fe make ΔT_{hys} decrease 0.9 K and 0.02 substitution of Mn make ΔT_{hys} decrease 0.3 K. It is well agreed with the reduction of ΔT_{hys} *of* 0.6 K in the sample M1F1, which equals to $0.5\cdot(0.3 + 0.9)$ K. Thus, value of ΔT_{hys} for $(Mn_{1.17-x}Fe_{0.73-y}V_{0.02})(P_{0.5}Si_{0.5})$ alloys can be tuned by mathematically designing the composition with the range of 0.6–1.5 K.

The magnetization as a function of the magnetic field for *M0F2* is shown in Fig. 1(*d*). To avoid the effect of thermal history and overestimated of entropy change for Fe_2P-type alloys, the isothermal magnetization has been measured using the method proposed by L. Caron et al. [25]. The magnetic hysteresis losses across T_C, determined by computing the areas between increasing and decreasing fields of magnetization (M) versus field ($\mu_0 H$) loop shown in Fig. 1 (*d*), are 8.6 and 2.8 J/kg for *M0F0* and *M0F2*, respectively. The magnetic hysteresis losses are comparable with the published data for the La–Fe–Si alloys with their transition near the boundary of the FOMT to SOMT [26]. The small thermal and magnetic hysteresis make the *M0F2* sample a promising candidate for future applications.

Rietveld refinement for XRD patterns of *M0F0* and *M0F2* measured at 373 K, where these samples should be both at the paramagnetic state, are illustrated in Fig. 2. The mains phase is identified to be hexagonal Fe_2P-typephase (space group P-62 m) and the impurity phase is identified to be $(Mn,Fe)_3Si$-type phase (space group Fm3m). As shown in Fig. 3

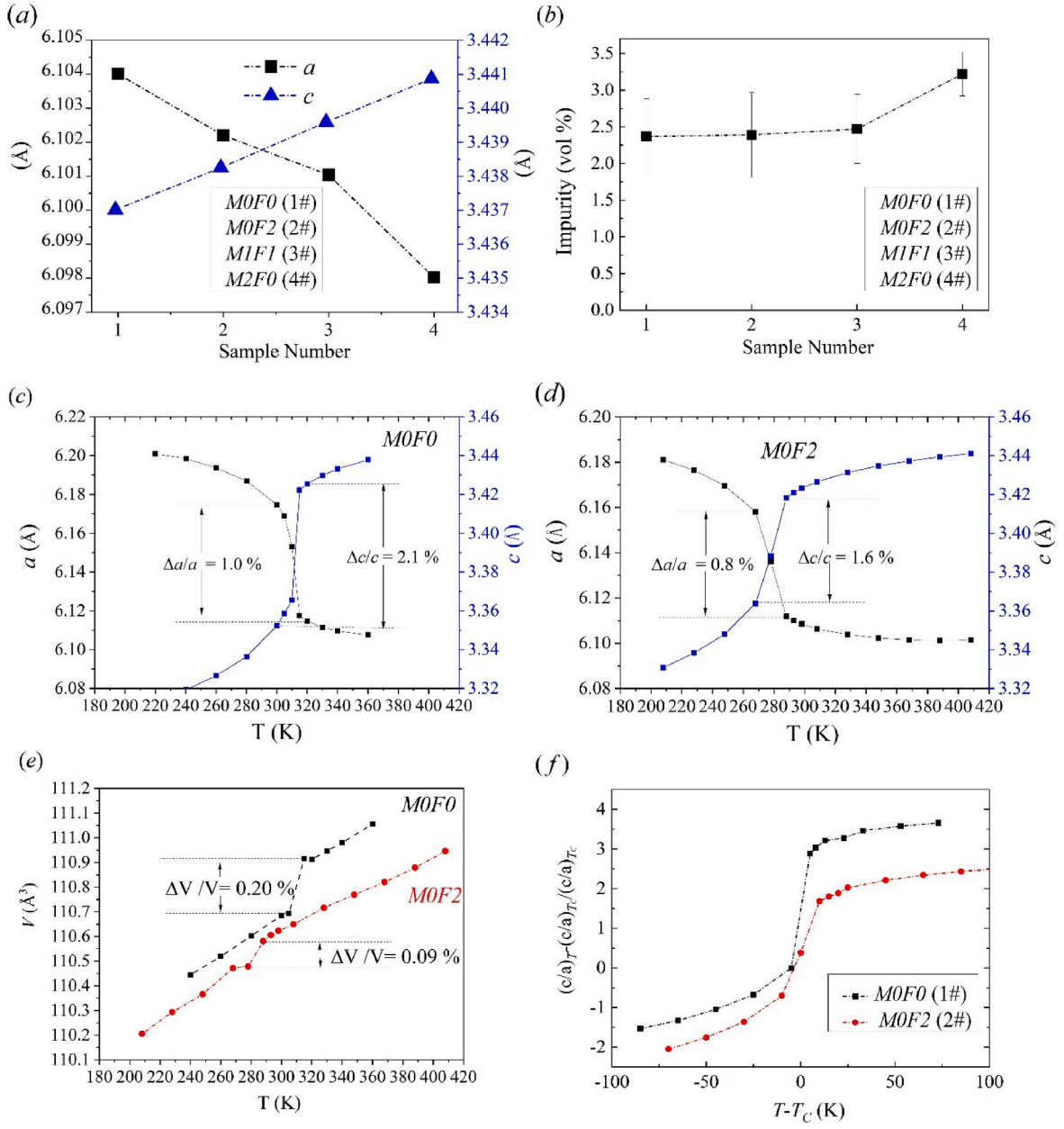

Fig. 3. (*a*) Lattice parameters *a* and *c*; (*b*) volume fraction of the impurity phase; (*c*) and (*d*) in-situ lattice parameters *a* and *c* as a function of the temperature; (*e*) unit cell volume as a function of temperature; (*f*) evolution of the (c/a) ratio of the cell parameters as a function of the temperature for the *M0F0* and *M0F2* alloys. The data are normalized with respect to the value at the transition temperature.

(a), the lattice parameters a decreases and c increase linearly with decreasing the phase transition temperature T_C. The value of T_C does not correlate to the increase in c/a ratio, which is due to the change in both the Mn and Fe content. The full substitution of V for Fe can result in a larger reduction of T_C compared to the full substitution of V for Mn, as shown in Table 1. The volume fractions of the 3:1 impurity phase determined from the XRD refinement are shown in Fig. 3(*b*). The high purity of the main phase (>97 vol%) helps to minimize the hysteresis caused by the pining effect of impurities [10].

To illustrating the crystal structure evolution during magneto-elastic transition, the in-situ XRD for *M0F0* and *M0F2* alloys, where temperature of environment is increasing from 180 K to 420 K, are measured and the lattice constants are extracted by Fullprof Rietveld refinement. The amplitude of the lattice changes for the *M0F0* and *M0F2* alloys, demonstrated in Fig. 3(*c*) and **(*d*)**, are $\Delta a/a = 1.0$ %, $\Delta c/c = 2.1$ % and $\Delta a/a = 0.8$ %, $\Delta c/c = 1.6$ %, respectively. The amplitude of the lattice changes is directly related to the strength of the FOMT and is consistent with the DSC and *M-T* results described above. The relative volume change ($\Delta V/V$) across the transition has been diminished by 55 % from 0.2 % to 0.09 %, see Fig. 3(*e*). The volume change introduces a volumetric stress, while the values of $\Delta a/a$ and $\Delta c/c$ contribute to an anisotropic stress as discussed for the MnFe(P, X) materials and a method for calculating the volumetric stresses and anisotropic stresses of Fe_2P-type alloys were provided by F. Guillou et al. [27]. The calculated volumetric stresses (σ_V) are 0.32 and 0.14 GPa, while the anisotropic stresses (σ_α) are 5.7 and 4.4 GPa for the *M0F0* and *M0F2* alloys, respectively. These two parameters for *M0F2* are comparable with the outstanding $MnFe_{0.95}P_{0.582}B_{0.078}Si_{0.34}$ alloy [27], which shows values of $\sigma_V = 0.15$ GPa and $\sigma_\alpha = 4.2$ GPa and has been proven to be mechanical stable. The difference between the respective lattice discontinuities of materials with FOMT concerns the jump on the ratio of the cell parameters c/a. To highlight this difference, the evolution of c/a ratio are

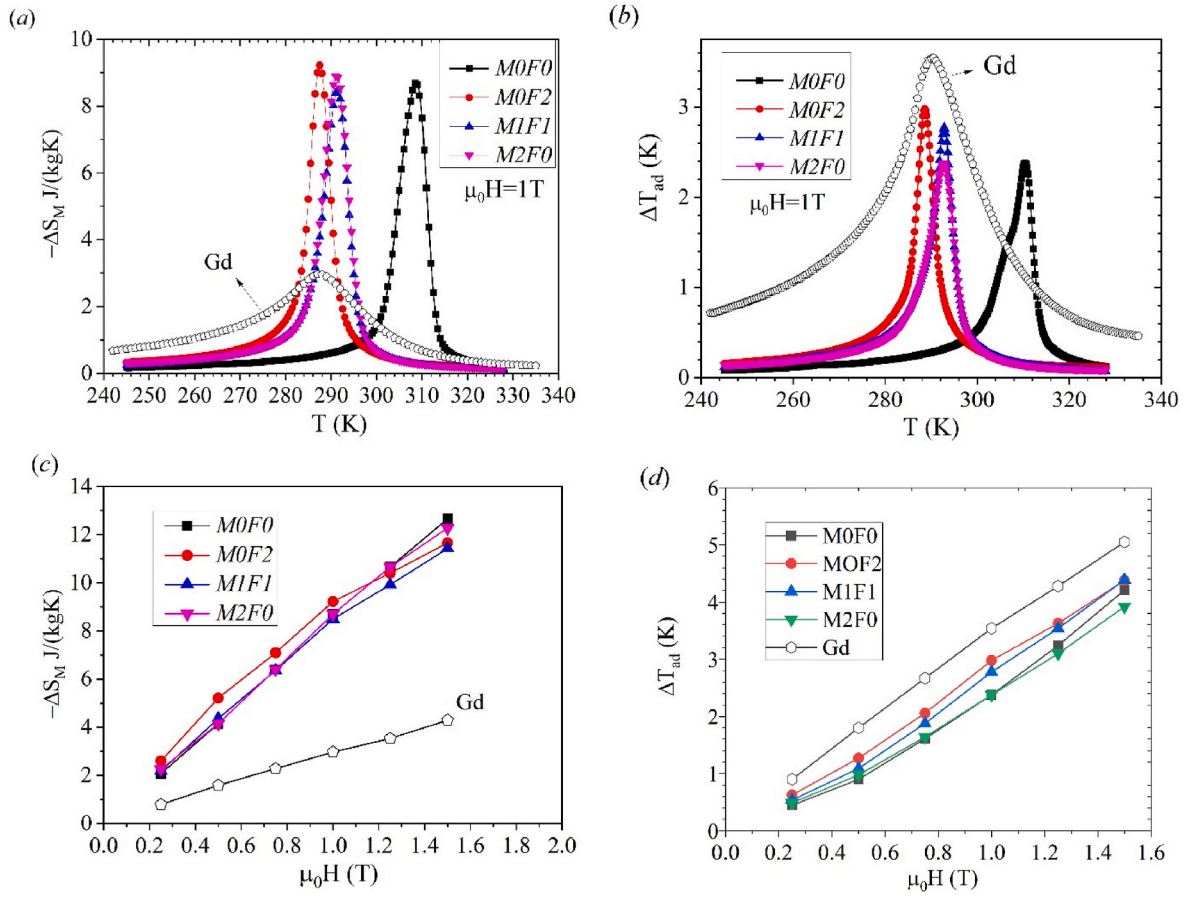

Fig. 4. (*a*) and (*b*) Temperature dependence of $|\Delta S_M|$ and ΔT_{ad} of the Gd and $Mn_{1.17-x}Fe_{0.73-y}V_{0.02}P_{0.5}Si_{0.5}$ alloys under a magnetic field change of 1 T from heat capacity measurement. (*c*) and (*d*) Field dependence of $|\Delta S_M|$ and ΔT_{ad} of the Gd and $Mn_{1.17-x}Fe_{0.73-y}V_{0.02}P_{0.5}Si_{0.5}$ alloys.

shown by using a normalisation in respect to the values for the ferromagnetic state at T_C [27]. As shown in Fig. 3(*f*), a lower value of $((c/a)_T\text{-}(c/a)_{Tc})/(c/a)_{Tc}$ is in line with the weakening of the FOMT in the *M0F2* alloy.

The value of the magnetic entropy change ($|\Delta S_M|$) of the alloys is an important criterion to evaluate how much energy can be converted by the magnetic field change. The value of the adiabatic temperature change (ΔT_{ad}) is an additional and more straightforward standard to evaluate the MCE [28]. The temperature dependence of $|\Delta S_M|$ and ΔT_{ad} for a field change of 0–1 T during heating are shown in Fig. 4(*a*) and 4 (*b*). ΔT_{ad} is measured in a Peltier cell based differential scanning calorimeter operating in a magnetic field (≤1.5 T) produced by a Halbach cylinder. The $|\Delta S_M|$ extracted by the in-field DSC measurements, and calculated from the heat capacity and entropy data [29], for *M0F2* in a magnetic field of 1.0 T is 9.2 J/(kgK). This value is consistent with the 9.1 J/(kgK) derived from iso-field magnetization curves based on Maxwell relations [21], as shown in the inset of Fig. 4(*a*). For the V substitution samples *M1F1* and *M2F0*, $|\Delta S_M|$ is strengthened, while ΔT_{ad} is weakened and vice versa, as shown in Fig. 4(*b*). However, for the *M0F2* alloy, both $|\Delta S_M|$ and ΔT_{ad} are strengthened. It shows different trends when the applied magnetic field increases to 1.25 and 1.5 T $|\Delta S_M|$ is 10.7, 10.4, 9.9 and 10.7 J/(kgK) under 1.25 T and is 12.7, 11.7, 11.4 and 12.3 J/(kgK) under 1.5 T for samples of *M0F0, M0F2, M1F1* and *M2F0*, respectively. If the magnetic field is increased to a higher field of 1.5 T $|\Delta S_M|$ of *M0F2* is lower than that of *M0F0*, as shown in Fig. 3(*c*). This can be understood from the fact that the *M0F2* alloy is saturated in a lower field compared to other samples, see Fig. 3(*c*), indicating a lower field to induce the FOMT. The value of dT_C/dB increases from 2.9 to 4.1 K/T for *M0F0* and *M0F2*. Consequently, *M0F2* has a larger $|\Delta S_M|$ value than the other samples for an applied magnetic field below 1.25 T.

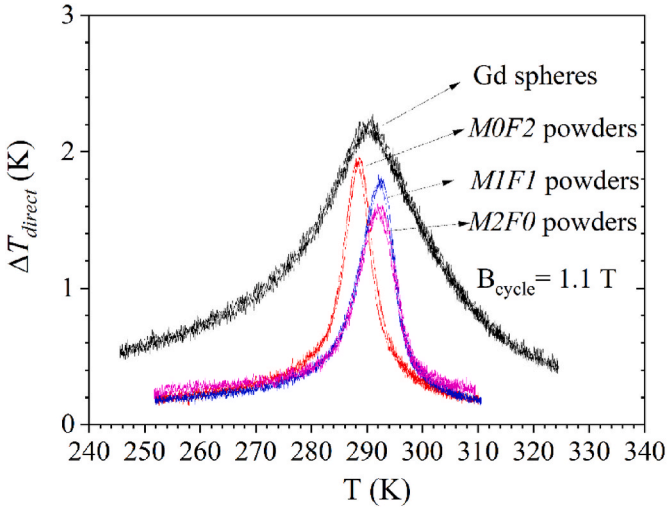

Fig. 5. Temperature dependence of ΔT_{direct} for the $La(Fe,Si)_{13}H_x$, $Ni_{46}Co_3Mn_{37}In_{10}Ge_4$, $Ni_{49}Mn_{37}In_{14}$, Gd and $Mn_{1.17-x}Fe_{0.73-y}V_{0.02}P_{0.5}Si_{0.5}$ alloys under a magnetic field of 1.1 T.

$(Mn,Fe)_2(P,Si)$ alloys crystallize. The FOMT originates from an electronic redistribution around the *3f* site, which is preferentially occupied by the Fe atoms. The *3g* site, which is preferentially occupied by Mn, does not show an instability in the electronic structure and magnetic moment. This effect has been termed 'mixed magnetism'. The mechanism of the better low field MCE of $Mn_{1.17}Fe_{0.71}P_{0.5}Si_{0.5}V_{0.02}$ alloys, i.e. M0F2 in this work, was from the enhanced M_{3f}, which is caused

Table 2
Values of ΔT_{direct} for the $Ni_{46}Co_3Mn_{37}In_{10}Ge_4$, $Ni_{49}Mn_{37}In_{14}$, $(La_{0.6}Ce_{0.4})_2Fe_{11}Si_2H_y$, Gd and $Mn_{1.17-x}Fe_{0.73-y}V_{0.02}P_{0.5}Si_{0.5}$ alloys near room temperature caloric cooling application.

Compounds	ΔT_{direct}/(K)	ΔH_{ap}/(T)	Ref.
$Ni_{46}Co_3Mn_{37}In_{10}Ge_4$	3.0	1.5	[35]
$Ni_{49}Mn_{37}In_{14}$	2.5	1.5	[36]
$(La_{0.6}Ce_{0.4})_2Fe_{11}Si_2H_y$	2.0	1.3	[37]
Gd	2.2	1.1	This work
$Mn_{1.17}Fe_{0.71}V_{0.02}P_{0.5}Si_{0.5}$	2.0	1.1	This work

by the enhancement of *3d-2p* hybridization or bonding on the *3f* site in the Fe_2P-type hexagonal structure when substituting 0.02 V with Fe content, which was concluded from the results of neutron diffraction and Mössbauer spectrum [23]. However, substitution of 0.02 V with Mn content (*M2F0*) shows a less effect on the low field performance, see Fig. 3 (c) and (d). It indicates that V atoms in the *M2F0* sample have a preference to enter the *3g* site. Thus, the atomic environment of *3d-2p* hybridization on *3f* site has been changed slightly in the *M2F0*.

The value of ΔT_{ad} for *M0F2* is 3.0 K in a field of 1 T, which is higher than the 2.5 K observed in the Mn–Fe–P–Si–B system (thin plates instead of powders) [8]. The inset of Fig. 4(*c*) illustrates the evolution of ΔT_{ad} for magnetic fields up to 2.0 T for *M0F2*. Compared to the reported maximum ΔT_{ad} values of 5.1 K for Gd metal [30], 5.8 K for La–Fe–Si–H plates [31] and 4.9 K for the $LaFe_{11.6-x}Mn_xSi_{1.4}H_y$ powders [10], *M0F2* has a competitive value of 5.6 K with a negligible thermal and magnetic hysteresis, which make it a promising novel MCE material for magnetic heat-pumping near room temperature.

Recently, not only remarkable MCE but also good reversibility during the cyclic field application is required. As shown in Fig. 5, ΔT_{direct} is 2.2, 2.0, 1.8 and 1.6 K for Gd, *M0F2, M1F1* and *M2F0*, respectively. Note that the in-field DSC results demonstrate that the maximum potential of the MCE is found at a rate of 3 K/min, while the direct adiabatic temperature change (ΔT_{direct}) estimates temperature change cycled at 0.1 Hz. These values of ΔT_{direct} are comparable to the performance in the $Mn_{1.19}Fe_{0.73}P_{0.49}Si_{0.51}$(M5) [32]. The reason of the derivation of ΔT_{direct} and ΔT_{ad} is because that ΔT_{direct} measurement is at the non-equilibrium condition while the ΔT_{ad} from heat capacity measurements is nearly equilibrium [33,34]. For instance, the value for Gd can show a variation of 0.8 K from the direct and indirect measurement [30]. The highest level of cyclic ΔT_{direct} had been demonstrated in Ni–Mn–In Heusler alloys by Zongbi Li. et al. [34,35] We compare the obtained magnetocaloric data with those in some other typical and promising alloys for caloric cooling application, like $Ni_{46}Co_3Mn_{37}In_{10}Ge_4$ [35], and $Ni_{49}Mn_{37}In_{14}$ [36], and La(Fe,Si)$_{13}H_x$ [37] compounds, as shown in Table 2. Herein, we provide both the value of ΔT_{direct} and ΔT_{ad} for the Gd and $Mn_{1.17-x}Fe_{0.73-y}V_{0.02}P_{0.5}Si_{0.5}$ alloys, which gives systematically and constructively data for choosing a promising candidate when building a magnetic heat-pumps.

4. Conclusion

A novel $Mn_{1.17-x}Fe_{0.73-y}V_{0.02}P_{0.5}Si_{0.5}$ material with a constant of 0.02 V and varying Fe and Mn concentrations has been explored. Thermal hysteresis could be tailored from 1.5, 1.2, 0.9, and 0.6 K for samples M0F0, M2F0, M1F1 and M0F2, respectively. During the first order magnetoelastic phase transition, the calculated volumetric stresses (σ_V) are reduced from 0.32 to 0.14 GPa for the *M0F0* and *M0F2* alloys. The sample *M0F2* shows a larger entropy change in the magnetic field range below the applied magnetic field of 1.25 T, which is caused by an improved dT_C/dB value and a decreased latent heat. For the optimal compound of sample *M0F2*, the MCE performance is characterized by a $|\Delta S_M|$ value of 9.1 J/(kgK) and a ΔT_{ad} value of 3.0 K in a field of 1 T with a low thermal hysteresis of 0.6 K, which paves the way to magnetocaloric materials that operate in low applied magnetic fields using the permanent magnets.

Declaration of competing interest

The authors declare the following financial interests/personal relationships which may be considered as potential competing interests:

Jiawei Lai reports financial support was provided by Guangzhou ethics project. Ekkes Bruck and Niels van Dijk have patent #P1600096NL00 pending to Technische Universiteit Delft. Jiawei Lai has patent #P1600096NL00 pending to Technische Universiteit Delft.

Acknowledgements

The authors acknowledge Anton Lefering, Kees Goubitz, and Bert Zwart for their technical assistance and Lian Zhang, J. Liu and Fengqi Zhang for discussion. This work has been financially supported by the Dutch national research organization NWO TTW under applied sciences project 14013. This work was supported by the Natural Science Foundation of China (Grant nos.: 12204181), Guangdong Basic and Applied Basic Research-Natural Science Foundation of Guangdong Province (Grant nos.: 2023A1515012962), Guangdong Provincial Key Laboratory of Optical Information Materials and Technology (No. 2017B030301007), Guangzhou Key Laboratory of Electronic Paper Displays Materials and Devices (No. 201705030007), National Center for International Research on Green Optoelectronics (No. 2016B01018), MOE International Laboratory for Optical Information Technologies and the 111 Project. M.M. acknowledges financial support from EIT Climate-KIC project “Local, magnetocaloric power conversion opportunities for Cities” (ID 210045).

References

[1] V.K. Pecharsky, K. Gschneidner Jr., Giant magnetocaloric effect in $Gd_5(Si_2Ge_2)$, Phys. Rev. Lett. 78 (1997) 4494.
[2] B.G. Shen, F.X. Hu, J.R. Sun, G.J. Wang, Z.H. Cheng, Very large magnetic entropy change near room temperature in LaFe11.2 Co0.7Si1.1, Appl. Phys. Lett. 80 (2002) 826–828.
[3] S. Fujieda, A. Fujita, K. Fukamichi, Large magnetocaloric effect in $La(FeSi)_{13}$ itinerant-electron metamagnetic compounds, Appl. Phys. Lett. 81 (2002) 1276.
[4] O. Tegus, E. Bruck, K.H. Buschow, F.R. de Boer, Transition-metal-based magnetic refrigerants for room-temperature applications, Nature 415 (2002) 150–152.
[5] E. Brück, O. Tegus, D.T.C. Thanh, K.H.J. Buschow, Magnetocaloric refrigeration near room temperature (invited), J. Magn. Magn Mater. 310 (2007) 2793–2799.
[6] E. Liu, W. Wang, L. Feng, W. Zhu, G. Li, J. Chen, H. Zhang, G. Wu, C. Jiang, H. Xu, F. de Boer, Stable magnetostructural coupling with tunable magnetoresponsive effects in hexagonal ferromagnets, Nat. Commun. 3 (2012) 873.
[7] J. Liu, T. Gottschall, K.P. Skokov, J.D. Moore, O. Gutfleisch, Giant magnetocaloric effect driven by structural transitions, Nat. Mater. 11 (2012) 620–626.
[8] F. Guillou, G. Porcari, H. Yibole, N. van Dijk, E. Brück, Taming the first-order transition in giant magnetocaloric materials, Adv. Mater. 26 (2014) 2671–2675.
[9] T.D. Brown, T. Buffington, P.J. Shamberger, Effects of hysteresis and Brayton cycle constraints on magnetocaloric refrigerant performance, J. Appl. Phys. 123 (2018), 185101.
[10] O. Gutfleisch, T. Gottschall, M. Fries, D. Benke, I. Radulov, K.P. Skokov, H. Wende, M. Gruner, M. Acet, P. Entel, M. Farle, Mastering hysteresis in magnetocaloric materials, Phil. Trans. Series A. Math. Phys. Eng. Sci. (2016) 374.
[11] N.H. Dung, L. Zhang, Z.Q. Ou, E. Brück, From first-order magneto-elastic to magneto-structural transition in (Mn,Fe)1.95P0.50Si0.50 compounds, Appl. Phys. Lett. 99 (2011), 092511.
[12] N.V. Thang, H. Yibole, N.H. van Dijk, E. Brück, Effect of heat treatment conditions on MnFe(P,Si,B) compounds for room-temperature magnetic refrigeration, J. Alloys Compd. 699 (2017) 633–637.
[13] J.W. Lai, Z.G. Zheng, B.W. Huang, H.Y. Yu, Z.G. Qiu, Y.L. Mao, S. Zhang, F.M. Xiao, D.C. Zeng, K. Goubitz, E. Brück, Microstructure formation and magnetocaloric effect of the Fe_2P-type phase in $(Mn,Fe)_2(P, Si, B)$ alloys, J. Alloys Compd. 735 (2018) 2567–2573.
[14] Z.Q. Ou, N.H. Dung, L. Zhang, L. Caron, E. Torun, N.H. van Dijk, O. Tegus, E. Brück, Transition metal substitution in Fe2P-based MnFe0.95P0.50Si0.50 magnetocaloric compounds, J. Alloys Compd. 730 (2018) 392–398.
[15] N.V. Thang, N.H.V. Dijk, E. Bruck, Tuneable giant magnetocaloric effect in $(Mn, Fe)_2(P,Si)$ materials by Co-B and Ni-B Co-doping, Materials 10 (2016).
[16] F. Guillou, H. Yibole, N.H. van Dijk, E. Brück, Effect of boron substitution on the ferromagnetic transition of $MnFe_{0.95}P_{2/3}Si_{1/3}$, J. Alloys Compd. 632 (2015) 717–722.

[17] N.V. Thang, H. Yibole, X.F. Miao, K. Goubitz, L. van Eijck, N.H. van Dijk, E. Brück, Effect of carbon doping on the structure and magnetic phase transition in (Mn, Fe)$_2$(P,Si)), JOM (J. Occup. Med.) 69 (2017) 1432–1438.
[18] N.V. Thang, X.F. Miao, N.H. van Dijk, E. Brück, Structural and magnetocaloric properties of (Mn,Fe)$_2$(P,Si) materials with added nitrogen, J. Alloys Compd. 670 (2016) 123–127.
[19] R.A. Kishore, S. Priya, A review on design and performance of thermomagnetic devices, Renew. Sustain. Energy Rev. 81 (2018) 33–44.
[20] R. Bjørk, A. Smith, C.R.H. Bahl, N. Pryds, Determining the minimum mass and cost of a magnetic refrigerator, Int. J. Refrig. 34 (2011) 1805–1816.
[21] K.A. GschneidnerJr, V.K. Pecharsky, A.O. Tsokol, Recent developments in magnetocaloric materials, Rep. Prog. Phys. 68 (2005) 1479–1539.
[22] F. Guillou, H. Yibole, G. Porcari, L. Zhang, N.H. van Dijk, E. Brück, Magnetocaloric effect, cyclability and coefficient of refrigerant performance in the MnFe(P, Si, B) system, J. Appl. Phys. 116 (2014), 063903.
[23] J. Lai, X. You, I. Dugulan, B. Huang, J. Liu, M. Maschek, L. van Eijck, N. van Dijk, E. Brück, Tuning the magneto-elastic transition of (Mn,Fe,V)$_2$(P,Si) alloys to low magnetic field applications, J. Alloys Compd. 821 (2020), 153451.
[24] X.-F. Miao, S.-Y. Hu, F. Xu, E. Brück, Overview of magnetoelastic coupling in (Mn, Fe)$_2$(P, Si)-type magnetocaloric materials, Rare Met. 37 (2018) 723–733.
[25] L. Caron, Z.Q. Ou, T.T. Nguyen, D.T. Cam Thanh, O. Tegus, E. Brück, On the determination of the magnetic entropy change in materials with first-order transition, J. Magn. Magn Mater. 321 (2009) 3559–3566.
[26] J.W. Lai, Z.G. Zheng, X.C. Zhong, R. Montemayor, Z.W. Liu, D.C. Zeng, Magnetocaloric effect of nonstoichiometric $La_{1-x}Fe_{11.4+x}Si_{1.6}$ alloys with first-order and second-order magnetic transitions, Intermetallics 63 (2015) 7–11.
[27] F. Guillou, H. Yibole, N.H. van Dijk, L. Zhang, V. Hardy, E. Brück, About the mechanical stability of MnFe(P,Si,B) giant-magnetocaloric materials, J. Alloys Compd. 617 (2014) 569–574.
[28] H. Yibole, F. Guillou, L. Zhang, N.H. van Dijk, E. Brück, Direct measurement of the magnetocaloric effect in MnFe(P,X)(X= As, Ge, Si) materials, J. Phys. Appl. Phys. 47 (2014), 075002.
[29] G. Porcari, F. Cugini, S. Fabbrici, C. Pernechele, F. Albertini, M. Buzzi, M. Mangia, M. Solzi, Convergence of direct and indirect methods in the magnetocaloric study of first order transformations: the case of Ni-Co-Mn-Ga Heusler alloys, Phys. Rev. B (2012) 86.
[30] M.D. Kuz'min, K.P. Skokov, D.Y. Karpenkov, J.D. Moore, M. Richter, O. Gutfleisch, Magnetic field dependence of the maximum adiabatic temperature change, Appl. Phys. Lett. 99 (2011), 012501.
[31] Y. Shao, J. Liu, M. Zhang, A. Yan, K.P. Skokov, D.Y. Karpenkov, O. Gutfleisch, High-performance solid-state cooling materials: balancing magnetocaloric and non-magnetic properties in dual phase La-Fe-Si, Acta Mater. 125 (2017) 506–512.
[32] T.V. Christiaanse, O. Campbell, P.V. Trevizoli, S. Misra, D. van Asten, L. Zhang, P. Govindappa, I. Niknia, R. Teyber, A. Rowe, A concise approach for building the diagram for Mn–Fe–P–Si hysteretic magnetocaloric material, J. Phys. Appl. Phys. 50 (2017), 365001.
[33] K.A. Gschneidner, V.K. Pecharsky, E. Brück, H.G.M. Duijn, E.M. Levin, Comment on "Direct measurement of the 'Giant' adiabatic temperature change in $Gd_5Si_2Ge_2$'', Phys. Rev. Lett. 85 (2000), 4190-4190.
[34] Z.G. Zheng, X.L. Chen, J.Y. Liu, H.Y. Wang, S. Da, Z.G. Qiu, D.C. Zeng, Dynamical response of Gadolinium in alternating magnetic fields up to 9Hz, Int. J. Refrig. 146 (2023) 100a–107a.
[35] J. Yang, Z. Li, X. Zhang, B. Yang, H. Yan, D. Cong, et al., Manipulation of thermal hysteresis and magnetocaloric effect in the Ni-Co-Mn-In alloys through lattice contraction: effect of Ge substitution for in, Acta Mater. 246 (2023), 118694.
[36] Z. Li, J. Yang, D. Li, Z. Li, B. Yang, H. Yan, et al., Tuning the reversible magnetocaloric effect in Ni-Mn-In-Based alloys through Co and Cu Co-doping, Adv. Electron. Mater. 5–3 (2019), 201800845.
[37] Y. Liu, X. Fu, Q. Yu, M. Zhang, J. Liu, Significant reduction of phase-transition hysteresis for magnetocaloric (La1-Ce)2Fe11Si2H alloys by microstructural manipulation, Acta Mater. 207 (2021), 116687.